

DOI: 10.21767/2470-9867.100030

Effect of Elemental Sulfur on Pitting Corrosion of Steels

Muthukumar Nagu*, Abdullatif Abdulhadi, Abdulrahman Huwaiji and Nayef M Alanazi

Research and Development Center, Saudi Aramco, Dhahran-31311, Saudi Arabia

*Corresponding author: Muthukumar Nagu, Research and Development Center, Saudi Aramco, Dhahran-31311, Saudi Arabia, Tel: 00966138726332; E-mail: muthukumar.nagu@aramco.com

Rec date: February 12, 2018; Acc date: March 03, 2018; Pub date: March 12, 2018

Copyright: © 2018 Nagu M, et al. This is an open-access article distributed under the terms of the Creative Commons Attribution License, which permits unrestricted use, distribution, and reproduction in any medium, provided the original author and source are credited.

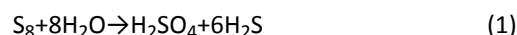
Citation: Nagu M, Abdulhadi A, Huwaiji A, Alanazi NM (2018) Effect of Elemental Sulfur on Pitting Corrosion of Steels. Insights Anal Electrochem. Vol.4 No.1:6

Abstract

This paper focuses on studying the pitting corrosion tendency of austenitic stainless steels (SS 316 L and NIT 60) and carbon steel (API 5 LX 60) in the presence of elemental sulfur. The pitting corrosion tendency of alloys was studied by using cyclic polarization technique at two different temperatures with and without elemental sulfur. Surface morphology and corrosion products formed on the exposed coupons were analyzed by scanning electron microscopy (SEM) and energy dispersive X-ray (EDX). It was found that the temperature played major role on pitting corrosion of alloys in presence of elemental sulfur. SS 316 L gave high pitting resistance than other tested alloys (NIT 60 and API 5 LX 60).

Keywords: Elemental sulfur; Pitting corrosion; Electrochemical method; SEM

deposition in natural gas transmission pipelines is immediately downstream of a point of pressure reduction which is also associated with temperature reduction [5]. Elemental sulfur (S_8) reacts with water at temperatures of greater than 80°C , resulting in significant acidification of the corrosion solution [6] as shown in **Equation 1**.



The previous experimental results also showed that steel was corroded severely when it has a direct contact with wet elemental sulfur at salt free conditions [7,8]. The most of researchers reported the gravimetric method to predict the elemental sulfur corrosion for natural gas pipeline application [6]. There is a limited publication on electrochemical methods to predict the pitting tendency of alloy in presence of elemental sulfur.

The aim of this paper is to use of cyclic polarization technique to study the pitting corrosion tendency of austenitic stainless steels (SS 316 L and NIT 60) and carbon steel API 5 LX 60 in presence and absence of elemental sulfur, with particular emphasis on detection of temperature effects, and identification of formed corrosion products.

Introduction

Sour gas fields have increasingly been explored and developed during the last decade due to the increasing energy demands [1]. Elemental sulfur deposition due to several chemical and physical facts indicates possibility of dissociation of hydrogen sulfide or polysulfide to produce elemental sulfur. Therefore dissociated elemental sulfur start to deposit in the form of small particles and adheres to the internal surface of pipelines. Elemental sulfur naturally acts as a cathode to the steel pipe due to the difference in their potential. An active electrochemical cell will be established as soon as free water or conductive condensates pass over the deposited elemental sulfur particle. When this happens, an accelerated localized corrosion will take place and initiate a pit [2-4]. The progression of this pit will be very unlikely to be arrested even if corrosion inhibitor is injected into the system [5]. Therefore, a leak of toxic and flammable gases will be expected in such location. The most common location for elemental sulfur

Experimental Procedure

GAMRY Interface 1000 was used for all electrochemical experiments. The electrochemical cell included a saturated calomel electrode (SCE) as a reference, a platinum counter electrode and the test sample as working electrode. The exposed surface area of the working electrode was 1 cm^2 . Open circuit potential and cyclic polarization experiments (ASTM Standard G 61) were conducted to determine the pitting tendency of the studied alloys in 3.5% sodium chloride solution with and without elemental sulfur. To study the temperature effect at low and high temperatures, 25°C and 80°C were selected in presence of three different steels namely: SS 316 L, NIT 60 and API 5 LX 60. The chemical compositions of the studied alloys are listed in **Table 1**. The elemental sulfur (about 0.5 gm) was deposited on the polished

tested coupons by heating it slightly above its melting-point (115°C - 120°C) then pouring it onto the coupon surface.

Table 1 Chemical composition of tested alloys.

Alloys	Cr	Ni	Mn	Mo	Si	N	C	P	S	Cu
SS 316 L	16-18	14 Max	2 Max	3 Max	0.75	0.01 Max	0.03	0.045 Max	0.03 Max	
Nitronic 60	16-18	9 Max	9 Max	0.75	4.00	0.08-0.18	0.10	0.04	0.01	0.75 max
API 5 LX.60							0.3	0.03	0.03	

The elemental sulfur deposited working electrode coupon was assembled in a glass autoclave electrochemical cell. The test solution (3.5% NaCl) was deaerated using nitrogen gas during the test period of 7 days and the open circuit potential was measured for entire test period. Cyclic polarization scan was then initiated at the end of the incubation period at scan rate of 0.125 mV/sec.

After the cyclic polarization experiments, Corrosion potential (E_{corr}), Pitting potential (E_{pit}), Repassivation potential (E_{rp}), overall pitting resistance (E_{RP}), and corrosion current (I_{corr}) values were obtained from the cyclic polarization curves. The tested coupons were removed after terminating the tests and characterized using scanning electron microscopy (SEM) and energy dispersive X-ray analysis (EDX). Corrosion products were then removed by treatment with Clarke solution [9] and the localized attack of the tested corrosion coupons were mapped by 3D DIKTAK surface profilometer. Finally, the overall

pitting resistance value was calculated using the following formula

$$\text{Overall pitting resistance}(E_{RP}) = \text{Repassivation potential}(E_{rp}) - \text{Corrosion potential}(E_{corr})$$

Results and Discussion

Cyclic polarization measurements were performed in order to determine the tendency of the tested samples to undergo localized pitting corrosion with and without elemental sulfur at 25°C and 80°C when placed in 3.5% NaCl solution. The derived electrochemical data from cyclic polarization experiments namely; Corrosion potential (E_{corr}), Pitting potential (E_{pit}), Repassivation potential (E_{rp}), overall pitting resistance (E_{RP}), and corrosion current (I_{corr}) values of each tested alloys at 80°C and 25°C, are presented in **Tables 2** and **3** respectively.

Table 2 Electrochemical data of various steels in 3.5% NaCl at 80°C.

Alloy	Elemental Sulfur (gm)	E_{corr} (mV)	E_{pit} (mV)	E_{rp} (mV)	Overall Pitting Resistance $E_{RP}=E_{rp}-E_{corr}$	I_{corr} ($\mu\text{A}/\text{cm}^2$)
SS 316 L	0	-265	111	-256	9	0.02
SS 316 L	0.5	-218	103	-454	-236	0.01
NIT 60	0	-253	-13	-268	-15	0.01
NIT 60	0.5	-581	NA	NA	NA	20
API 5 LX 60	0	-904	NA	NA	NA	3.5
API 5 LX 60	0.5	-985	NA	NA	NA	22

Table 3 Electrochemical data of various steels in 3.5% NaCl solution at 25°C.

Alloy	Elemental Sulfur (gm)	E_{corr} (mV)	E_{pit} (mV)	E_{rp} (mV)	Overall Pitting Resistance $E_{RP}=E_{rp}-E_{corr}$	I_{corr} ($\mu\text{A}/\text{cm}^2$)
SS 316 L	0	-300	421	-297	3	0.01
SS 316 L	0.5	-204	338	-400	-196	0.01
NIT 60	0	-222	177	-280	-58	0.02
NIT 60	0.5	-581	39	-365	-222	0.01
API 5 LX 60	0	-869	NA	NA	NA	0.3
API 5 LX 60	0.5	-726	NA	NA	NA	400

Electrochemical behavior of SS 316 L

Figure 1a and **1b** show the cyclic polarization curves obtained in the deaerated 3.5% sodium chloride solution at 25°C and 80°C. Both the tested temperatures, SS 316 L showed the passive region, where the passive range decreased in presence of elemental sulfur, indicating that the passive properties of the films slightly degraded as the temperature increased. Furthermore, the overall pitting resistance value of SS 316 L (E_{RP}) at 25°C (**Table 3**) with sulfur was more negative (-196 mV) than in the absence of sulfur system (3 mV). It indicated that SS 316 L was not able to reform the passive film during the reverse scan (**Figure 1b**) at 80°C. There was no much change in the corrosion current (I_{corr}) values in presence and absence of sulfur at both 80°C and 25°C.

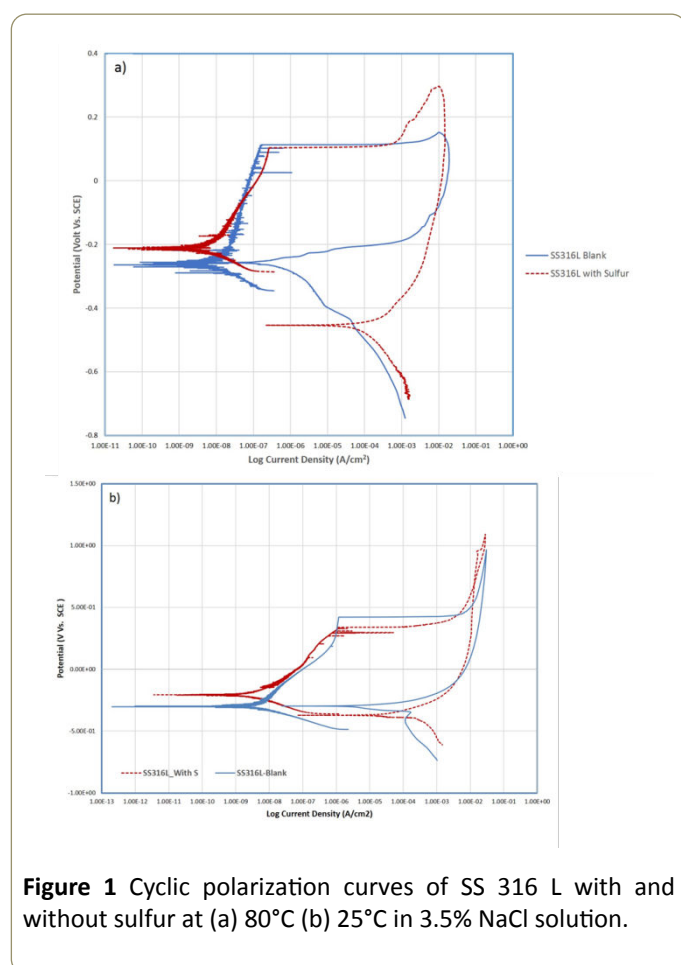


Figure 1 Cyclic polarization curves of SS 316 L with and without sulfur at (a) 80°C (b) 25°C in 3.5% NaCl solution.

The morphologies of the pits also showed a significant change at high temperature in presence of elemental sulfur, as shown in **Figures 2** and **3**.

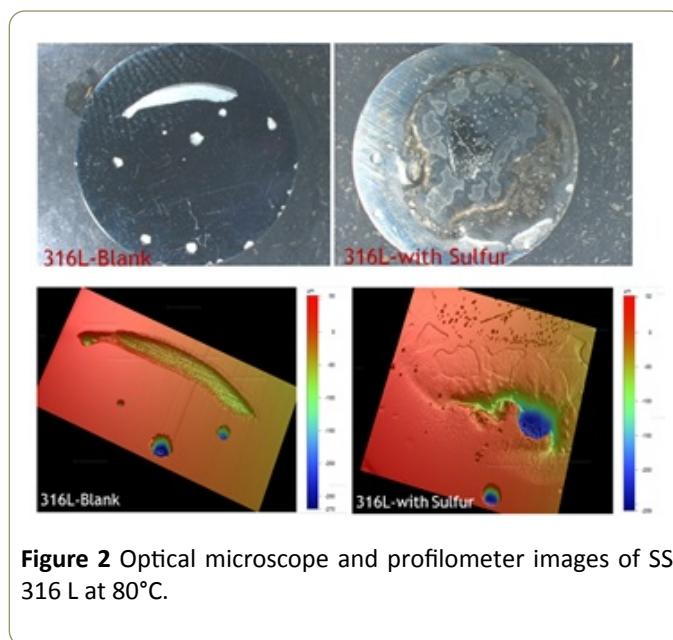


Figure 2 Optical microscope and profilometer images of SS 316 L at 80°C.

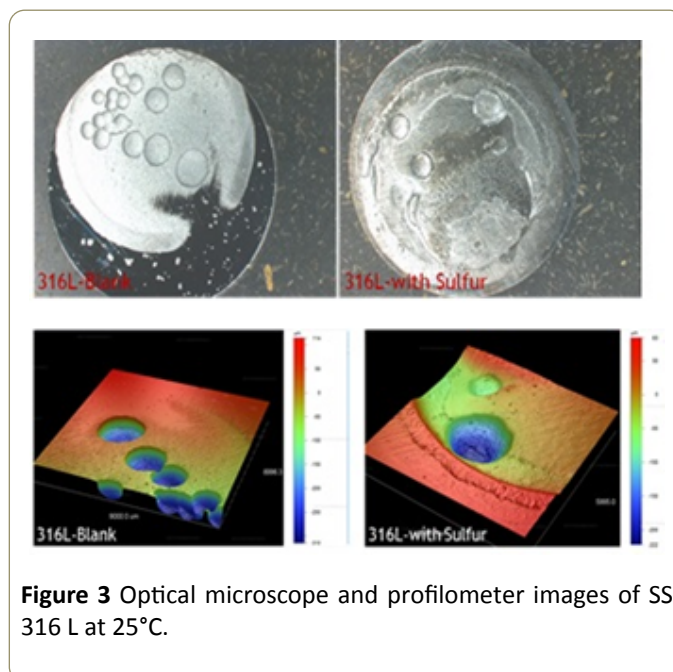


Figure 3 Optical microscope and profilometer images of SS 316 L at 25°C.

Stainless steel surfaces are generally rendered passive by formation of a surface oxides layer. This layer depends on the effective concentration of chromium, nickel and molybdenum at the surface of the metal phase [10]. Damaging or destroying the passive layer will result in pitting and shifting the corrosion potential [11]. For instance, the tested austenitic stainless steel samples (SS 316 L and NIT 60) showed nobler potential compared to carbon steel API 5 LX 60.

There are three mechanisms of pitting corrosion has been discussed [12,13] that focus on (1) passive film penetration (2) film breaking (3) adsorption. Scattered and isolated pits (**Figures 2** and **3**) were observed in the control substrate (i.e., without sulfur, blank) at both temperatures (80°C and 25°C) while in the presence of elemental sulfur, the morphology of the developed pits were changed to cover all the exposed area. The measured deepest pit was 247 μm and the width

was 1.8 mm at 80°C. Examining the tested coupon at 80°C after terminating the experiment with elemental sulfur deposition confirmed the reaction of elemental sulfur with the substrate. The collected SEM images (**Figures 4 and 5**) revealed the presence of iron and sulfur on the substrate, whereas, sodium chloride crystal deposition on the SS 316 L coupons surface in blank experiment.

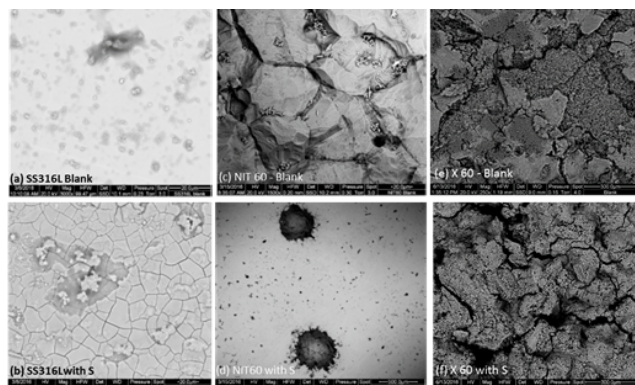


Figure 4 SEM images of SS 316 L, NIT 60 and X 60 alloys at 80°C.

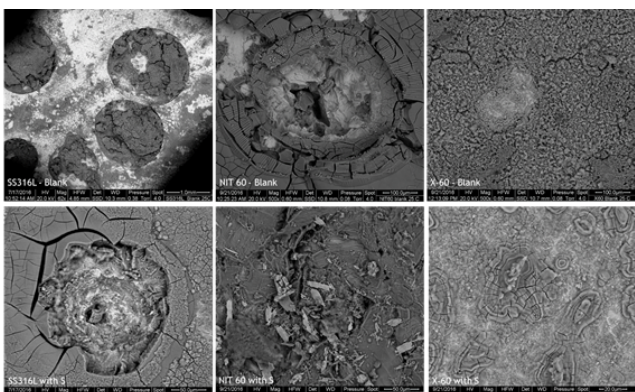


Figure 5 SEM images of SS 316 L, NIT 60 and X 60 alloys at 25°C.

Electrochemical behavior of NIT 60

On the other hand, the elemental sulfur deposition on NIT 60 shifted the corrosion potential to more negative potential at 80°C (-581 mV) compared to the control sample (-253 mV). It indicated that the passive film was completed disturbed by elemental sulfur (**Figure 6a**). Furthermore the cyclic polarization curve exhibited different behavior at lower temperature as illustrated in **Figure 6b**. Based on hysteresis loop and overall pitting tendency value (E_{RP}) of NIT 60, presence and deposition of elemental sulfur on the substrate resulted in greater pitting tendency than in the absence of elemental sulfur (**Figure 6b**, **Tables 2 and 3**). There was clear indication on pitting potential value change in presence of sulfur system at both temperatures. At 25°C, the pitting potential of NIT 60 was decreased from 177 mV to 39 mV

without and with sulfur respectively. Such behavior might be attributed to the lower content of the Nickel and Molybdenum alloying elements in NIT 60 alloy [14]. The corrosion current (I_{corr}) increased from 0.01 $\mu\text{A}/\text{cm}^2$ to 20 $\mu\text{A}/\text{cm}^2$ in presence of sulfur added system at 80°C. But in the case of 25°C data, there was no much change in the corrosion current. It reveals that the temperature plays a major role on dissolving the passive film on the NIT 60 substrate by sulfur hydrolysis reaction [6].

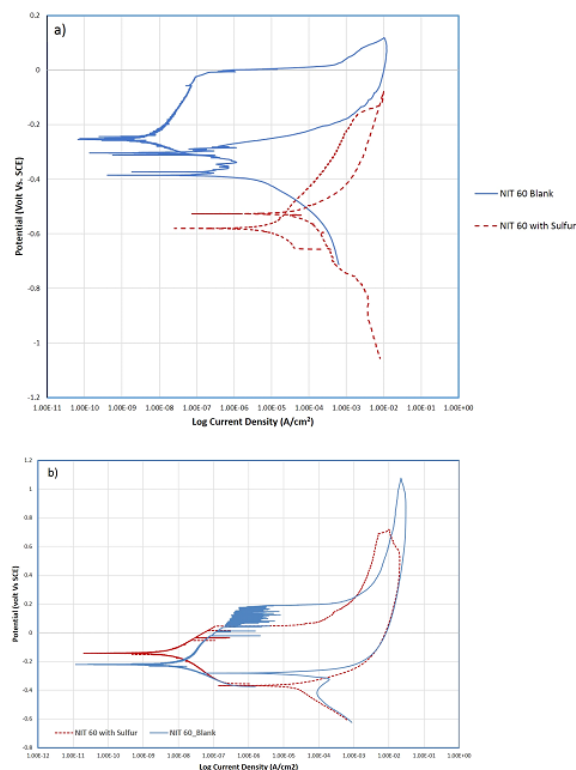


Figure 6 Cyclic polarization curves of NIT 60 with and without sulfur at (a) 80°C (b) 25°C in 3.5% NaCl solution.

Less dense scattered pits were observed in the control NIT 60 substrate (blank) while in the presence of elemental sulfur, the morphology of the developed pits covered larger areas. The measured deepest pit was 108 μm and the width was 2.2 mm at 80°C. SEM/EDS diagnostic detected copper leaching at the grain boundaries in the blank sample (**Figures 4 and 7**) at 80°C. Iron and sulfur peaks were also observed in presence of elemental sulfur with NIT 60 system (**Figures 4 and 8**).

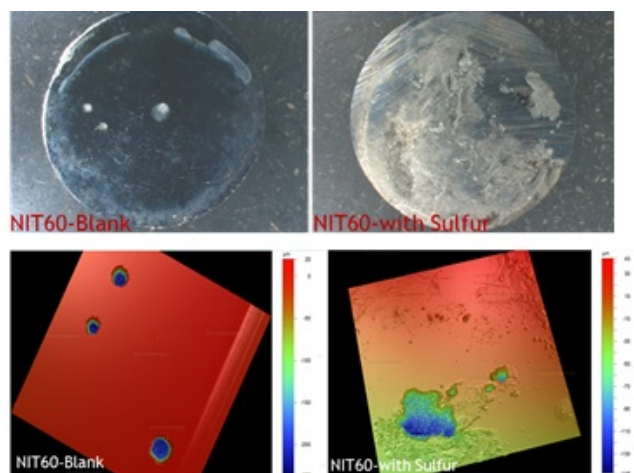


Figure 7 Optical microscope and profilometer images of NIT 60 at 80°C.

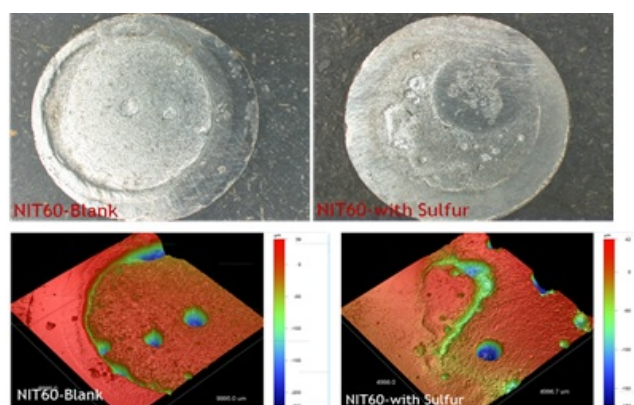


Figure 8 Optical microscope and profilometer images of NIT 60 at 25°C.

Electrochemical behavior of API 5 LX-60

There was no passive layer due to the absence of effective concentrations of passivation alloying elements in case of carbon steel API 5 LX-60. Cyclic polarization curves at the tested temperatures indicated the active corrosion process in both systems with and without sulfur. The deposited elemental sulfur at 80°C reacted with carbon steel substrate and shifted the open circuit and resulted in increasing the current density (**Figure 9** and **Table 3**). The corrosion potential of API 5 LX 60 was moved to lower potential in presence of elemental sulfur (-985 mV) compared to absence of sulfur system (-904 mV). In general, reactivity of the deposited elemental sulfur and the corrosion current densities increased at elevated temperature. There was no passive layer and it clearly indicated the active corrosion process in both the system (with and without sulfur), where the corrosion current density increases with increasing potential (**Figure 9** and **Table 2**).

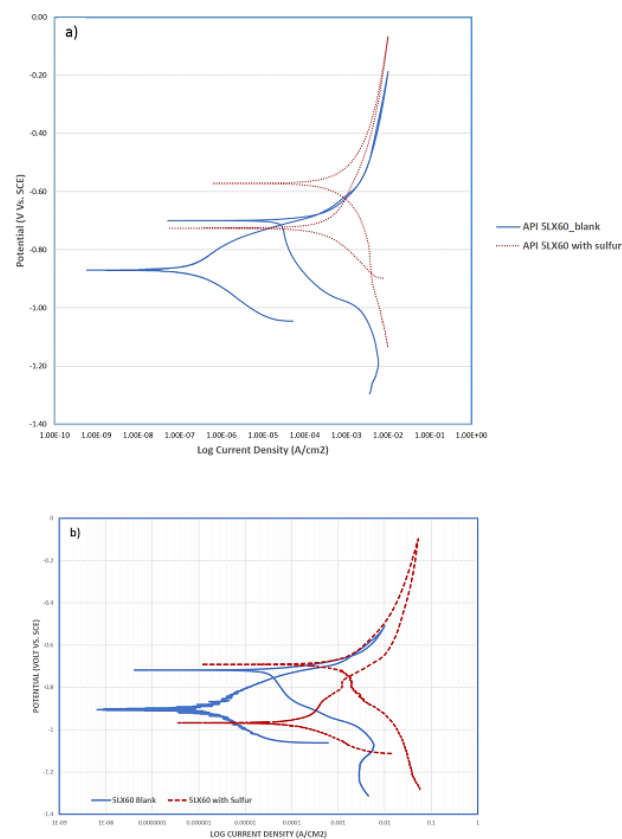


Figure 9 Cyclic polarization curves of API 5 LX-60 with and without sulfur at (a) 80°C (b) 25°C in 3.5% NaCl solution.

The corrosion current was increased significantly in presence of elemental sulfur at 25°C compared to 80°C (3rd order difference) in NaCl solution. The substrate suffered from general corrosion in the control substrate while in the presence of elemental sulfur, the damage mechanism shifted to severe localized corrosion covering all the exposed area (**Figures 10** and **11**). In presence of sulfur, the measured deepest pit was 487 μm (shallow pit) at 80°C experiments. Iron and oxygen peaks were noticed in carbon steel API 5 LX 60 substrate without sulfur system (Blank, **Figures 4** and **5**). Iron and sulfur peaks were noticed on API 5 LX 60 substrate in presence of sulfur added system.

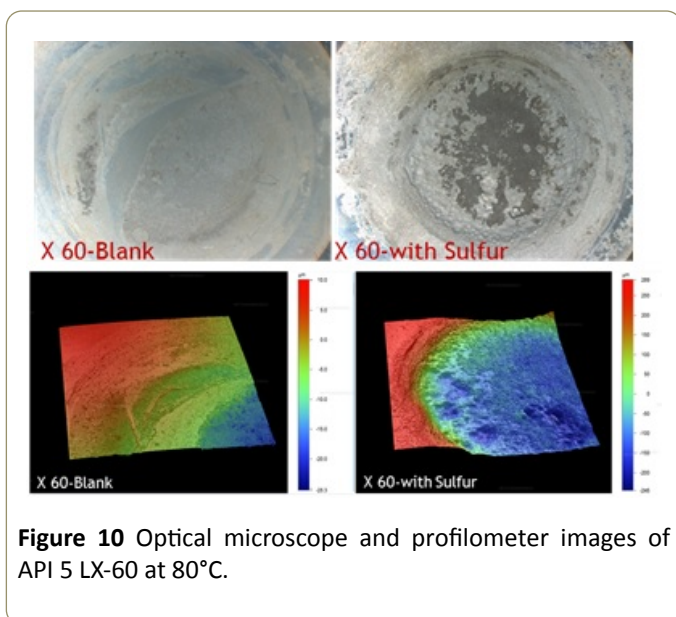


Figure 10 Optical microscope and profilometer images of API 5 LX-60 at 80°C.

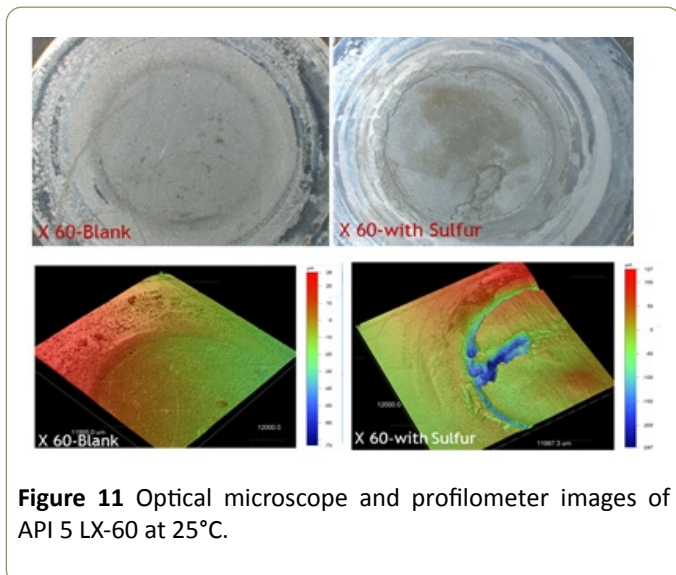


Figure 11 Optical microscope and profilometer images of API 5 LX-60 at 25°C.

Discussion

From the above results, the corrosion potential of API 5 LX 60 was moved to more negative potential compared to other tested stainless steels (SS 316 L and NIT 60). The temperature plays a major role on pitting corrosion of the tested alloys in presence of elemental sulfur. The major observations from the cyclic polarization experiments at two different temperatures can be summarized as follows: a rapid decrease in pitting potential with NIT 60 at 80°C, An increase in corrosion current densities and significant changes in pit morphologies with increasing temperature. However, there was not much change in pitting potential with SS 316 L at 80°C. It indicates that SS 316 L has more pitting resistance than NIT 60 at 80°C. In case of API 5 LX 60, the higher corrosion current was observed at 25°C than 80°C. The pitting corrosion tendency of the tested alloys increases with increasing temperature (80°C) compared to room temperature (25°C). It was reported that the elemental sulfur enhances the corrosion processes at high temperature through sulfur hydrolysis reaction [6].

3D profilometer studies of stainless steels (SS 316 L and NIT 60) and carbon steel API 5 LX 60 with and without sulfur system (**Figures 10** and **11**) exhibited that the pit depths were very high in presence of sulfur added system. The corrosion damage mechanism changed with increasing temperature from a uniform attack to severally localized one. Among the three different alloys, carbon steel showed the highest level of shallow pit corrosion attack on the substrate.

Elemental sulfur corrosion process with water was described as autocatalytic in carbon steel [3,7,14,15]. Smith et al. reported that the dry solid sulfur does not produce corrosion of carbon steel [16]. It is only when moisture is present that sulfur induces corrosion. In addition, pH of the solution, temperature and presence of chlorides are significant contributors to the corrosion of steels in S-containing environments [6,17-21]. Temperature plays major role on sulfur corrosion reaction through sulfur hydrolysis [7]. The present study also confirmed that temperature played a major role on elemental sulfur corrosion of steels in presence of elemental sulfur through sulfur hydrolysis. Sulfur hydrolysis was higher at high temperatures [6,22]. Smith et al. reported that direct contact between steel and elemental sulfur is necessary for catastrophic corrosion to occur [23]. It can be seen that in the presence of chlorides and elemental sulfur there is a limiting temperature for each alloy that is largely related to the Molybdenum content [24]. The corrosion reactions in presence of elemental sulfur are as follow:

Oxidation



Reduction



Overall



In summary, SS 316 L showed better pitting resistance than other tested two alloys (NIT 60 and API 5 LX 60). It might be due to the high concentration of Mo, Ni in SS 316 L austenitic steel [11]. The pitting resistance ranking of tested alloys: SS 316 L > NIT 60 > API 5 LX 60.

Conclusion

The current work investigated the effect of elemental sulfur on the pitting corrosion tendency of three different steels in 3.5% sodium chloride solution. The results indicate that:

1. Successfully demonstrated the use of cyclic polarization technique to predict the pitting corrosion tendency of three different steels in presence and absence of elemental sulfur.
2. SS 316 L showed higher pitting resistance than other two tested steels. The pitting resistance of alloys: SS 316 L > NIT 60 > API 5 LX 60

3. Iron and sulfur peaks were observed as a passive film in presence of sulfur experiments in all three tested alloys at both temperatures. Cyclic polarization data demonstrated good agreement with the calculated pitting resistance equivalent number (PREN) for the studied alloys.

4. The temperature played major role on pitting corrosion of alloys in presence of elemental sulfur (Sulfur hydrolysis).

Acknowledgement

The author gratefully acknowledges the support of Saudi Aramco for granting permission to publish this paper. Also, they would like to thank Advanced Analysis Unit, Saudi Aramco for their support on SEM/ EDX analysis.

References

- Sun H, Wen J, Schmidt P, Hudgins R (2012) Study of Elemental Sulfur Corrosion And Inhibition Using Taguchi Method And Orthogonal Arrays. NACE International, Houston, Texas, USA.
- Wilken G (1996) Effect of Environmental Factors on Downhole Sour Gas Corrosion. NACE International, Houston, Texas, USA.
- Schmitt G (1991) Effect of Elemental Sulfur on Corrosion in Sour Gas Systems. *Corrosion* 47: 285-308.
- Cezac P, Serin JP, Reneaume JM, Mercadier J, Moutonb G (2008) Elemental sulphur deposition in natural gas transmission and distribution networks. *J Sup Flu* 44: 115-122.
- Pack DJ (2005) 'Elemental sulphur' Formation in natural gas transmission pipelines. Paper Presented at the 14th Biennial Joint Technical Meeting on Pipelines Research, Berlin, Germany pp: 1-14.
- Fang, H, Brown B, Young D, Nescic S (2011) Investigation Of Elemental Sulfur Corrosion Mechanisms. NACE International, Houston, Texas, USA.
- Macdonald D, Roberts B, Hyne JB (1978) The Corrosion of Carbon Steel by Wet Elemental Sulfur. *Corros Sci* 18: 411-425.
- Fang H, Young D, Nescic S (2008) Elemental Sulfur corrosion of Mild Steel at High Concentrations of Sodium Chloride. 17th International Corrosion Congress, Paper #2592, Las Vegas, NV, USA.
- ASTM G1-03 (2017) Standard Practice for Preparing, Cleaning, and Evaluating Corrosion Test Specimens, ASTM International, West Conshohocken, Pennsylvania.
- Leckie HP, Uhlig HH (1966) Environmental Factors Affecting the Critical Potential for Pitting in 18-8 Stainless Steel. *J Electrochem Soc* 113: 1262.
- Horvath J, Uhlig HH (1968) Critical Potentials for Pitting Corrosion of Ni, Cr-Ni, Cr-Fe, and Related Stainless Steels. *J Electrochem Soc* 115: 791-795.
- Strehblow HH, Korros W (1976) Mechanisms of Pitting Corrosion in Corrosion Mechanisms in Theory and Practice. New York, USA, p: 792.
- Strehblow HH, Marcus, Oudar J (1995) Corrosion mechanisms in theory and practice. New York, USA, p: 221.
- Scully JC (1990) The Fundamentals of Corrosion. 3rd Ed. Pergamon Press, Oxford, USA, p: 212.
- Nasirpouri F, Mostafaei A, Fathyunes L, Jafari R (2014) Assessment of localized corrosion in carbon steel tube-grade AISI 1045 used in output oil-gas separator vessel of desalination unit in oil refinery industry. *Engg Fail Anal* 40: 75-88.
- Smith L, Craig B (2005) Practical Corrosion Control measures for Elemental Sulfur containing Environment. CORROSION/ 2005, Paper no. 05646 (Houston, TX: NACE, 2005).
- Ho-Chung-Qui DF, Williamson AI (1987) Corrosion experiences and inhibition practices in wet sour gas gathering systems, USA.
- Fang H, Young D, Nescic S (2008) Elemental sulfur corrosion of mild steel at high concentration of sodium chloride. In Proceedings of the 17th International Corrosion Congress, Las Vegas, NV, USA, pp: 1-16.
- Steudel R (1996) Mechanism for the Formation of Elemental Sulfur from Aqueous Sulfide in Chemical and Microbiological Desulfurization Processes. *Ind Eng Chem Res* 35: 1417-1423.
- Okonkwo PC, Shakoor RA, Benamor A, Amer Mohamed AM, Al-Marri MJ, et al. (2017) Corrosion Behavior of API X100 Steel Materials in a Hydrogen Sulfide Environment. *Metals* 7: 109.
- Zhang GA, Yu N, Yang LY, Guo XP (2014) Galvanic corrosion behavior of deposit-covered and uncovered carbon steel. *Corros Sci* 86: 202-212.
- Fang H, Young D, Nescic S (2008) Corrosion of mild steel in the presence of elemental sulfur. CORROSION/ 2008, Paper No. 08637 (Houston, TX: NACE International, 2007).
- Smith L, Craig B (2008) Corrosion mechanisms and material performance in environments containing hydrogen sulfide and elemental sulfur. SACNUC Workshop 22nd and 23rd October, Brussels.
- Khaksar L, Shirokoff J (2017) Effect of Elemental Sulfur and Sulfide on the Corrosion Behavior of Cr-Mo Low Alloy Steel for Tubing and Tubular Components in Oil and Gas Industry. *Materials* 10: 430.